Received: 4 February 2022 | Revised: 22 December 2022 | Accepted: 1 January 2023

DOI: 10.1002/wsb.1430

RESEARCH ARTICLE

WILDLIFE SOCIETY BULLETIN Open Access

Using cost-effectiveness analysis to compare density-estimation methods for large-scale wildlife management

Zackary J. Delisle[1] | Patrick G. McGovern[1] | Brian G. Dillman[2] | Carson J. Reeling[3] | Joe N. Caudell[4] | Robert K. Swihart[1]

[1]Department of Forestry and Natural Resources, Purdue University, 195 Marsteller Street, West Lafayette, IN 47907, USA

[2]Department of Aviation Technology, Purdue University, West Lafayette, IN 47907, USA

[3]Department of Agricultural Economics, Purdue University, West Lafayette, IN 47907, USA

[4]Indiana Department of Natural Resources, Bloomington, IN 47401, USA

Correspondence
Zackary J. Delisle, Department of Forestry and Natural Resources, Purdue University, 195 Marsteller Street, West Lafayette, IN 47907, USA.
Email: zdelisle@purdue.edu

Funding information
Indiana Department of Natural Resources, Grant/Award Number: W-48-R-02

Abstract

Density estimates for animal populations often inform conservation and management decisions. Many methods to estimate animal density exist but deciding between competing alternatives traditionally has depended upon assessing multiple factors (e.g., precision, total cost, area sampled) independently and often in an ad hoc manner. Cost-effectiveness analysis is a tool that economists use to decide objectively between competing alternatives. We extend cost-effectiveness analysis to simultaneously integrate precision and per-area cost of sampling when selecting between competing techniques used to estimate animal density both after a single application of a method and across several applications of capital equipment. Our extension allows for weighting of factors that may vary with the objectives and constraints of decision makers. We apply our extension of cost-effectiveness analysis to a case study in which population density of white-tailed deer (*Odocoileus virginianus*) was estimated in 3 large management units in Indiana, USA, using 3 competing distance-sampling methods: fecal-pellet, camera-trap, and aerial sampling. The unweighted cost effectiveness of aerial sampling with color and infrared sensors was usually superior after a single application of each method and was always superior across several applications in differing landscapes. Pellet sampling was the most cost effective after a single application of each method in an agriculturally-dominated management unit. Although camera sampling has increased in popularity, the cost effectiveness of camera sampling was poorer than the other 2 methods, even when allowing for potential future innovations to streamline data processing. Cost-effectiveness analysis can be useful when selecting among competing methods for monitoring animal populations of conservation and management importance. The same principles used in our cost-effectiveness analysis can be used to decide between competing alternatives related to any ecological monitoring in addition to density estimation.

KEYWORDS

aerial sampling, animal conservation, camera sampling, camera trap, decision making, fecal-pellet sampling, vertical-looking infrared, wildlife management

Wildlife management benefits from estimates of animal density that are precise, cost-effective, and representative of the actual population (Williams et al. 2002). Such density estimates can inform conservation and management decisions that regulate harvest (Devers et al. 2021, Tombre et al. 2022), diminish animal-induced habitat degradation (Spake et al. 2020), minimize wildlife-human conflict (Conover 2001, Hussain et al. 2007), update the protection status of rare species and critical habitat (Meylan and Donnelly 1999, Hawkins and Racey 2005), and mitigate demographic responses to habitat or climate change (Péron et al. 2012, Lewis et al. 2015). Agencies often must implement conservation and management decisions across large, functional jurisdictional units that span hundreds to thousands of km^2 (Sinclair 1991, Thiemann et al. 2008, Wallace et al. 2010) and thus require methods of density estimation that are applicable to large spatial extents.

When managers consider potential methods for estimating animal density, the utility of those methods often depends upon multiple factors including monetary costs and performance of the density estimator (Lyra-Jorge et al. 2008, De Bondi et al. 2010, Laguardia et al. 2021). Monetary costs include capital costs (Glover-Kapfer et al. 2019), recurring expenditures from sampling operations (De Bondi et al. 2010), and labor required for data processing (Delisle et al. 2021, Palencia et al. 2021). The performance of a density-estimation method can be assessed by the total area over which density is inferred (Laguardia et al. 2021) and the relative precision of the resulting density estimate (Campbell et al. 2004). Although desired, bias is extremely difficult to assess for density estimates of wildlife populations. Generally, factors associated with monetary costs and performance pertain to cost effectiveness. In economic analyses, cost effectiveness is routinely presented as the ratio of the cost of an alternative in dollars and some measure of performance of that alternative (Boardman et al. 2011).

Numerous studies have compared methods for estimating animal density (Parmenter et al. 2003, Urbanek et al. 2012, Anile et al. 2014, Keiter et al. 2017) but focused primarily on separately comparing the precision and total cost associated with different methods. Other published comparisons of methods for estimating animal density have referred to the total cost or total effort of a method as a measure of cost effectiveness. Therefore, as an aid to resource managers, we extend simple methods of cost effectiveness analysis borrowed from economics to decide between competing techniques used to estimate animal density. We then apply cost-effectiveness analysis to evaluate 3 different field techniques to estimate the density of white-tailed deer (*Odocoileus virginianus*) across 3 large management units in Indiana, USA, during late winter in 2021. Specifically, we assess the cost effectiveness of fecal-pellet, camera-trapping, and aerial methods using distance-sampling estimators. We also evaluate if and how cost effectiveness differed for each method as a function of landscape composition.

METHODS

Cost-effectiveness analysis

Cost effectiveness, CE, is the ratio of the cost, C, of an alternative and some measure of performance (i.e., effectiveness), E, of that alternative (Boardman et al. 2011), expressed as $CE = C/E$. Because wildlife managers often desire density estimates across large areas over which management is implemented, cost per unit land area, C/a, is a relevant measure of costs. Consistent with past research, area, a, is the total area over which density is inferred (Laguardia et al. 2021). Similarly, wildlife managers strive for density estimates that are precise to facilitate detection of changes in density across repeatedly sampled areas and yield more confidence in single estimates. Given this, a relative measure of precision, e.g., the inverse of the coefficient of variation (CV), is often the only measure of effectiveness of interest regarding a method to estimate animal density (Skalski et al. 2005). Therefore, a cost-effectiveness ratio (sensu Boardman et al. 2011, p. 465) for this situation can be expressed as

$$CE = \frac{C/a}{1/CV} \tag{1}$$

which is simply the cost per unit land area standardized by relative precision. Cost is the total cost of the alternative, including the capital cost of equipment and the recurring cost associated with collecting, processing, and analyzing the data. When deciding among competing methods for estimating density, the most cost-effective alternative is the method with smallest cost effectiveness. Feasibility constraints on C (e.g., maximum allowance for personnel hiring or vehicle purchasing) or minimum required precision (i.e., maximum allowance for CV) can be set *a priori* to remove alternatives that do not meet the minimum standards of an agency.

Management often benefits from knowledge of spatiotemporal changes in density or abundance rather than a single density estimate in time and space (Schaub and Kéry 2021). Consequently, many agencies estimate density on a recurring seasonal or yearly basis, and thus invest in what is hoped to be long-lived equipment. We therefore calculate C as an annuity, or an annualized total cost. Formally, we assume that (1) capital equipment (e.g., camera traps, aerial sampling equipment) is purchased at cost CC and will last N applications, (2) there are recurring costs for each application of the method (e.g., labor to collect, process, and analyze the data), and (3) the same measure of precision $1/CV$ is returned and area a sampled for each application of the method. In this case, the resulting annualized cost is

$$C = CC/A(r, N) + FOC + DPC \tag{2}$$

where FOC = field-operating cost per application, DPC = data-processing cost per application, $A(r, N) = [(1 + r)^N - 1]/[r(1 + r)^N]$ = the annuity factor (Campbell and Brown 2016), and r = a discount rate. We specify r at 0.03, which is approximately equal to the real social rate of time preference in the U.S. and is consistent with federal guidance on the choice of discount rate for economic analysis (Office of Management and Budget 2003). Formally, this is the rate at which individuals are willing to postpone a present consumption in exchange for future consumption and hence represents one measure of the opportunity cost or shadow value of invested funds. Effectively, $A(r, N)$ takes a large up-front capital expenditure and annualizes the capital expenditure, i.e., converts the capital expenditure into an annual expenditure such that, if you were to take the present value of all expenditures over the N applications of the capital's life at a discount rate of r, then it would equal CC.

We recognize that the relative importance of factors contributing to a method's cost effectiveness could vary due to the management objective as well as political, financial, or bureaucratic constraints acting on a management agency. To explicitly allow for variation in relative importance, we modified Equation 1 to allow for user-specified weights, denoted by w, for cost-effectiveness input parameters such that

$$CE_{anw} = \frac{\left(\frac{CC}{A(r,N)} * w_{CC} + FOC * w_{FOC} + DPC * w_{DPC}\right) \Big/ (a * w_a)}{(1/CV) w_{CV}} \tag{3}$$

where w_p, $p \in \{CC, FOC, DPC, a, CV\}$ = manager-specified weights for each parameter. To determine weights, an importance score, i_p, ranging from 0 (no importance) to 100 (critically important), can be given to each parameter in Equation 3. Then a compositional weight for parameter p is given by $w_p = \frac{p i_p}{\sum_{p=1}^{P} i_p}$. When $w = 1$ for all P parameters, Equation 3 simplifies to Equation 1.

Case study

Study area

We conducted sampling during the late winter of 2020–2021 in Regional Management Units (RMU) 3, 4, and 9 in Indiana, USA (Figure 1; Swihart et al. 2020). Weather regimes in each RMU followed a 4-season temperate pattern. Regional Management Unit 3 (10,233 km^2) was predominantly row-crop agriculture (8,113 km^2), with intermittent patches of forest and grasslands (1,446 km^2) and was located within the Central and Eastern Corn Belt Plains ecoregions (U.S. Environmental Protection Agency 1997). Soils were predominantly silty loams. Within patches of forest, common tree species included black cherry (*Prunus serotina*), black oak (*Quercus velutina*), black walnut (*Juglans nigra*), pin oak (*Q. palustris*), sassafras (*Sassafras albidium*), and white oak (*Q. alba*), and common herbaceous species included black snakeroot (*Sanicula marilandica*), enchanter's nightshade (*Circaea lutetiana*), garlic mustard (*Alliaria petiolata*), sweet cicely (*Osmorhiza claytonii*), and Virginia knotweed (*Polygonum virginianum*). Private property comprised 98.4% of the total area in RMU 3.

Unlike RMU 3, RMU 4 (16,187 km^2) was predominantly forested (9,208 km^2), contained far less agricultural land (3,141 km^2), and was located within the Interior Plateau, Interior River Valleys and Hills, and Eastern Corn Belt Plains ecoregions (U.S. Environmental Protection Agency 1997). Soil types in the western two-thirds of RMU 4 were bedrock soils with sandstone, limestone, and siltstone, whereas soils in the eastern third were primarily silty loams. Forests were primarily mesic hardwoods that contained American beech (*Fagus grandifolia*), black oak, sugar maple (*Acer saccharum*), tulip poplar (*Liriodendron tulipifera*), and white oak. Dominant herbaceous species included common blue violet (*Viola sororia*), enchanter's nightshade, honewort (*Cryptotaenia canadensis*), jack-in-the-pulpit (*Arisaema triphyllum*), and wild licorice (*Galium circaezans*). Private property comprised 88.1% of the total area in RMU 4.

Lastly, RMU 9 (4,716 km^2) was a mixture of forests (400 km^2), wetlands (607 km^2), and row-crop agriculture (2,663 km^2), and was located within the Southern Michigan/Northern Indiana Drift Plains and Eastern Corn Belt Plains ecoregions (U.S. Environmental Protection Agency 1997). Soil types included silty and sandy loams, neutral clays, and muck soils. Forest patches ranged from mesic to hydric hardwoods that contained American basswood (*Tilia americana*), black cherry, red maple (*A. rubrum*), sugar maple, and silver maple (*A. saccharinum*). Dominant herbaceous species included black snakeroot, common blue violet, enchanter's nightshade, garlic mustard, and Virginia knotweed. Private property comprised 97.4% of the total area in RMU 9.

Within each RMU, we focused aerial sampling within 41.44-km^2 areas that we randomly selected from Indiana's deer harvest reporting grid. The reporting grid spans the entirety of each RMU, and spatially separates

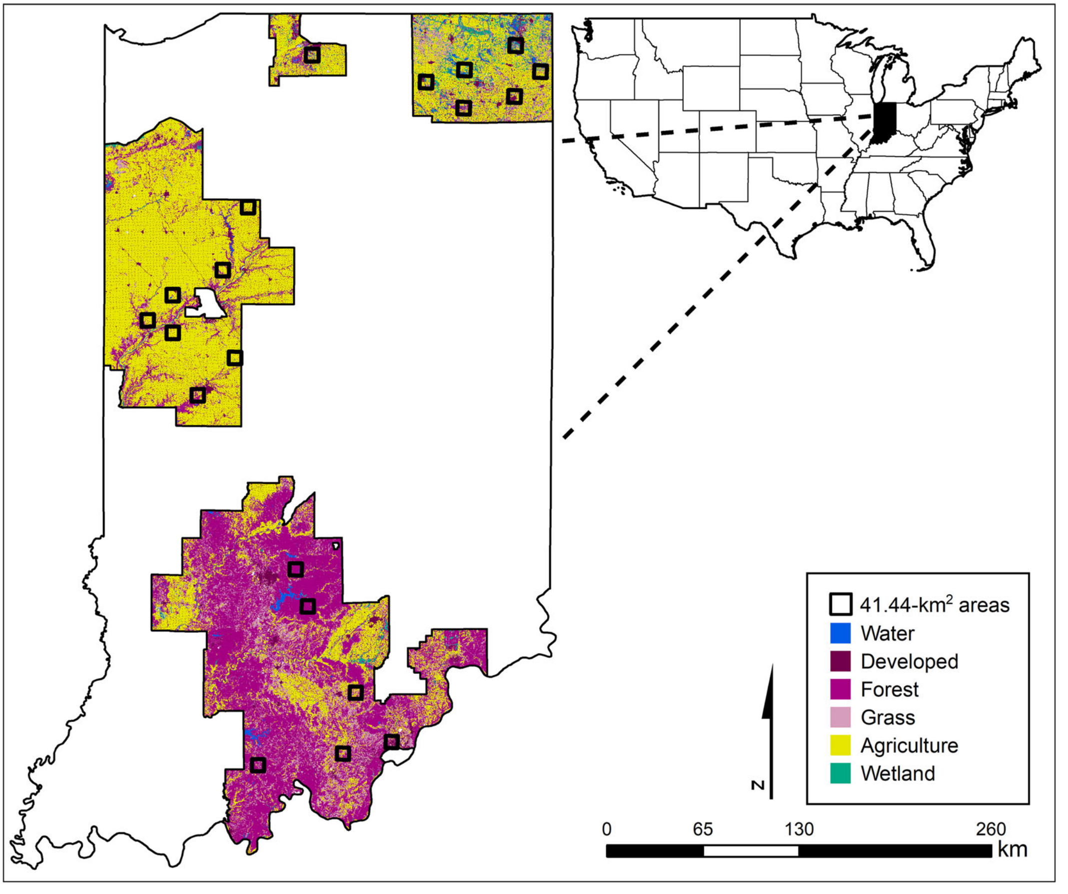

FIGURE 1 Land cover types within deer Regional Management Units 3 (west central), 4 (southern), and 9 (northeastern) in Indiana, USA. The 41.44-km^2 areas where we conducted fecal-pellet, camera-trap, and aerial sampling for white-tailed deer in Spring 2021 are shown within Regional Management Units.

each RMU into 6.44 × 6.44 km areas from which the Indiana Department of Natural Resources records deer harvests. For fecal-pellet and camera-trap sampling, we sampled 10.36-km^2 square sub-areas (henceforth referred to as sub-areas) placed within the larger 41.44-km^2 areas in which we conducted aerial sampling. We placed sub-areas to ensure that habitat composition was reflective of the greater 41.44-km^2 area and that property access across the sub-area was as homogeneously distributed as possible. In total, we sampled 7, 6, and 7 different areas within RMUs 3, 4, and 9, respectively. The number of areas we sampled in each RMU was dependent on a larger project with aims of estimating deer density across each RMU by sampling several additional years and areas.

Modelling methods

We estimated density using conventional distance sampling (Buckland et al. 2001) for each of the 3 methods we evaluated. To ensure robust estimation of density, we presented the relevant consideration for each assumption in the methods section below. For each method, we estimated density in both open (defined as agricultural fields, pasture, and herbaceous grasslands) and concealed (defined as wetlands and forest) habitats in each RMU. Total density for each method across both open and concealed habitats in each RMU was estimated using a weighted geographic stratification as $\hat{D}_y = \sum_{i=1}^{2}\left(\frac{H_{iy}}{H_y}\right)\hat{D}_{iy}$ where $\hat{D}_y$ is the density estimate across both habitats in RMU y, H_{iy} is the total area of habitat i in RMU y, H_y is the total area of both habitats in RMU y, $\hat{D}_{iy}$ is the habitat-specific density estimate in RMU y, and $var(\hat{D}_y) = \sum_{i=1}^{2}\left(\frac{H_{iy}}{H_y}\right)^2 var(\hat{D}_{iy})$.

Fecal-pellet sampling

Sampling of fecal pellets is a common method used to estimate the densities of many wildlife species (Wood 1988, Barnes 2001, Marques et al. 2001, Todd et al. 2008). To sample for fecal-pellet groups of white-tailed deer, we surveyed 200-m line transects during 1–24 March 2021 across the 3 RMUs. The assumption that fecal-pellet groups were detected at their initial location was easily met as fecal-pellet groups are stationary. Transect location and orientation was determined randomly using ArcMap 10.7 (ESRI, Redlands, CA, USA), subject to the dual constraints of property access and separation from the nearest neighboring transect by ≥200 m. Random placement ensured that we met the assumption that fecal-pellet groups were distributed independently of the transect. We sampled concealed habitat disproportionate to its availability because white-tailed deer spend less time in agricultural fields compared to areas of natural cover (Beier and McCullough 1990, Nixon et al. 1991). Studies utilizing pellet transects in adjoining states were used to guide decisions on transect spacing and number (Urbanek et al. 2012, Anderson et al. 2013). Details of our stratified sampling are provided in Delisle et al. (2022*b*).

During field sampling, each transect was surveyed by one of multiple surveyors who conducted fecal-pellet sampling. A single surveyor walked each transect twice to meet the assumption that objects on the line are detected with certainty. During the first pass, the surveyor focused all attention directly on the transect line to ensure perfect detection at distance 0. During the second pass, the surveyor focused attention to each side of the line. Upon detection of a fecal-pellet group, each surveyor recorded the perpendicular distance from the transect line to the center of the fecal-pellet group, which met the assumption that distances were measured accurately. If a fecal-pellet group was detected on the first pass, the group was removed so that no fecal-pellet group was accidentally counted twice on the second pass; thus, the assumption that detections are independent events was met.

To estimate deer density in concealed and open habitats using fecal-pellet sampling, we used the formula from Marques et al. (2001) and methods in Delisle et al. (2022*b*). To estimate the persistence time for dung piles deposited during the study period in each RMU, we used the interobserver method from Delisle et al. (2022*b*). Specifically, we used a weighted habitat-specific persistence rate for each RMU, with weights based on the sampling effort in each habitat type in each sub-area (Estimation of persistence, available in Supporting Information). We used the same defecation rate of 26.8 fecal-pellet groups/deer/day for density estimates in each RMU (Delisle et al. 2022*b*). We included variation from the persistence rate but not the defecation rate in the final density estimates from pellet sampling because we did not experimentally estimate the defecation rate. Instead, we used the defecation rate from previous research in similar study areas (Delisle et al. 2022*b*). Similarly, to model the detection process and select a final model, we used the methods in Delisle et al. (2022*b*). We fit all detection functions using the Distance package in R (Miller 2021).

Camera-trap sampling

Camera-trap sampling is a popular method used to estimate animal density (Delisle et al. 2021). We deployed Browning Strike Force HD (Browning Trail Cameras, Birmingham, AL, USA) motion-triggered camera traps from 2 February to 15 March 2021. We strived to deploy 20 camera traps per sub-area, which Buckland et al. (2001) recommended as the minimum number of sampling locations to estimate the encounter-rate variance. However, access to private property limited the number of cameras in some sub-areas. We randomly selected camera-trap locations using ArcMap 10.7 subject to the same access and proximity constraints as fecal-pellet transects, which met the assumption that deer were distributed independently of camera locations. In wooded areas, we affixed camera traps to trees at a height of 1 m and in areas without trees we affixed camera traps to t-posts at 1-m height. Affixing cameras at a height of 1 m assured that we would meet the assumption of detecting deer at distance 0 with certainty, as deer could not pass beneath the camera. We oriented all camera traps to face north to avoid sun glare at dawn and dusk. In rare instances, locations of camera traps were slightly altered from random (<20 m) to ensure a suitable location. When triggered, camera traps captured a burst of 3 photos usually separated by 0.3 seconds. We set minimum time delays between triggers to 1 or 5 seconds. Quickly triggering upon detection helped ensure that deer were detected at their initial location.

To estimate deer density in each RMU and habitat type (concealed and open) using camera traps, we relied on the distance-sampling method of Howe et al. (2017):

$$\hat{D} = \frac{2t\sum_{k=1}^{K} n_k}{\Theta d^2 \sum_{k=1}^{K} T_k \widehat{Pr_k}} * \frac{1}{\hat{A}} \tag{4}$$

In Equation 4, $\hat{D}$ = estimated density, k = the camera trap sampled, n_k = the total detections at camera trap k, t = the time interval between consecutive detections (sec), Θ = the angle of view (radians) of the camera trap, d = the truncation distance (m), T_k = the total time sampled (sec), $\widehat{Pr_k}$ = the probability of detection in the camera-trap sampling area at a given t demarcated by Θ and d, and $\hat{A}$ = the estimated fraction of a camera-trap day spent active and thus available for camera-trap sampling. For our application, we most often measured the distance to a deer in the first photo contained within a burst, and therefore we used t = 1.6 or 5.6 sec for most cameras. To estimate $\hat{A}$ of white-tailed deer in each RMU, we first used the average anchoring method from Vazquez et al. (2019) to double-anchor deer detection times by the average sunset and sunrise times across the spatiotemporal extent of our sampling in each RMU. We then estimated $\hat{A}$ by fitting circular kernel distributions to the double-anchored detection times using the methods of Rowcliffe et al. (2014) and estimated the standard error (SE) of $\hat{A}$ with nonparametric bootstrapping (Rowcliffe et al. 2014) using the activity package in R (Rowcliffe 2021). Like conventional multipliers, the resulting SE for $\hat{A}$ was propagated into the SE of $\hat{D}$ using the delta method (Buckland et al. 2001).

We estimated distances from the camera trap to deer in photos by using reference videos of deployers holding signs that indicated their distance from the camera trap at the edges and center of the camera trap's field-of-view (Howe et al. 2017), which helped to meet the assumption that distances were measured accurately. To estimate a detection function, we fit half-normal key functions with either 2 Hermite polynomial adjustments or no adjustments, uniform key functions with either 1 or 2 cosine adjustment, and hazard-rate key functions with either no, 1 or 2 cosine adjustments. Additionally, we fit half-normal and hazard-rate key functions with several different combinations of factor covariates including the following: (1) whether the camera trap's flash fired upon detection (night vs day), (2) local microhabitat surrounding the camera trap (same microhabitats as in fecal-pellet sampling), (3) RMU, (4) RMU and camera-trap flash, (5) camera-trap flash and microhabitat, (6) RMU and microhabitat, and (7) camera-trap flash, microhabitat, and RMU. We estimated the SE of $\hat{D}$ using nonparametric bootstrapping to sample camera traps with replacement. Similar to fecal-pellet sampling, we fit all detection functions using the Distance package in R (Miller 2021).

We measured distances to the same deer in consecutive photo bursts, as is standard with camera-trap distance sampling. Because recording distances to the same individual introduces overdispersion and violates the assumption of independent detections, we used the 2-step procedure proposed by Howe et al. (2019) for model selection. Specifically, we used Akaike's Information Criterion adjusted for overdispersion (QAIC) to select the best model within the same key function. We used the average number of detections per individual per camera visit as a measure of the overdispersion factor, $\hat{c}$. After selecting the best model within key functions, we selected the best overall model by dividing the χ^2 goodness-of-fit (GOF) statistic by the degrees of freedom of the model. We chose the key function with the lowest quotient as the best model. To determine whether to fit a pooled detection function across both open and concealed habitat types, or to fit unique detection functions for open and concealed habitat types, we compared the sum of the QAIC from the best models (according to the 2-step process) fit separately and the QAIC of the best pooled detection function.

Aerial sampling

Aerial sampling has been used to estimate population abundance of many wildlife species (Haufler et al. 1993, Jachmann 2002, Winiarski et al. 2014, Stapleton et al. 2016). In the context of distance sampling, counts obtained from visual surveys on aerial platforms assume perfect detection along either the transect line or the distance at which left truncation is specified (Laake et al. 2008). We used a vertical-looking infrared (VLIR) platform coupled with high-resolution color video in an attempt to meet this assumption more readily than when sampling with observers counting from the sides of fixed-wing aircraft (Caughley and Grice 1982, Fleming and Tracey 2008) or when using forward-looking infrared (FLIR) cameras that increase distance and vegetative obstruction between the thermographer and animals (Bernatas and Nelson 2004, Storm et al. 2011, Smith et al. 2020). Vertical-looking infrared permits detection of deer directly beneath the aerial platform (Kissell and Nimmo 2011). Combining VLIR with high-resolution color video was adopted to further augment VLIR capabilities (Franke et al. 2012, Chrétien et al. 2016).

We conducted aerial sampling during daylight hours from 8 February to 10 March 2021. During our flights, we flew 16, ~6.44-km transects that were aligned north to south in each 41.44-km^2 area. Based on prior work with deer, each transect was separated by 400 m (Kissell and Nimmo 2011). Transects were systematically aligned but randomly placed, ensuring that deer were distributed randomly in relation to the transects. We flew at an altitude of ~450 m and speed of ~65 mph in a Sky Arrow Light Sport Aircraft (Magnaghi Aeronautica S.p.A., Naples, Italy) to minimize the chance of deer movement in response to the aircraft. Altitude was restricted to 300 m in some 41.44-km^2 areas due to low cloud cover. The width of the field-of-view of the camera was 126.5 m and 84.3 m for flights conducted at 450 m and 300 m above ground altitude, respectively, and thus there was never overlap between neighboring transects. We never documented reactive movement towards the aircraft, and our flight speeds minimized the potential for random double counting, which poses no problem for population monitoring (Buckland et al. 2001). To that end, estimators of the encounter-rate variance are robust to violation of the assumption that detections are independent (Buckland et al. 2015), which could arise from double counting.

We recorded VLIR video of the ground beneath the plane with an IR-TCM HD 1024 stationary thermography camera combined with a telephoto 60 mm lens (Jenoptik, Jena, Germany). Simultaneously, we recorded vertical-looking, red-green-blue (RGB) video of the same areas using a Nikon D810 DSLR camera combined with the Nikon AF DC-NIKKOR 135 mm f/2D lens (Nikon Inc., Melville, NY, USA). Cameras were affixed to either side of the aircraft and pointed directly at the ground during flight. The VLIR and RGB video were synchronously recorded, georeferenced, and stored digitally using a GeoDVR Mini (Remote GeoSystems Inc., Fort Collins, CO, USA) and Garmin GPS (Garmin Ltd., Olathe, KS, USA).

After we conducted our flights, we viewed the VLIR and RGB video using the LineVision—Ultimate software (Remote GeoSystems, Inc.). Upon detecting a heat signature in the VLIR video that we suspected to be a deer, RGB video was used for confirmation. In addition, we measured the perpendicular distance from each deer to the centerline of the video and recorded whether the deer was located in concealed or open habitat. The LineVision software is equipped with a feature that allows measuring of distance, which ensured that we measured distances accurately. Similar to other past research using VLIR (Kissell and Nimmo 2011), after preliminary examination of the aerial sampling distance data, we found uniform detection across all distances from the transect line to the field-of-view edge of the camera (Aerial detection probability, available in Supporting Information; Delisle et al. 2022*a*). However, we did document false negatives caused by viewers missing infrared signatures (i.e., perception errors; Brack et al. 2018). Therefore, we estimated the probability of a single viewer detecting an infrared signature, and the standard error of that probability, using the mark-recapture methods described in Delisle et al. (2022*a*) on a subset of our aerial data from each altitude.

We estimated deer density in each RMU and habitat (open and concealed) by using the equation from Buckland et al. (2015) with the probability of detecting an infrared heat signature as a multiplier:

$$\hat{D} = \frac{n}{Q} * \frac{1}{pr\,(det)} \tag{5}$$

where n = the total number of deer detected, Q = the total area sampled, and $pr\,(det)$ = the probability of detecting an infrared heat signature. We used the probabilities of detecting a deer in each RMU from Delisle et al. (2022*a*). We calculated Q with the field-of-view of the infrared sensor and the above-ground altitude maintained by the pilot. We used the field-of-view of the infrared sensor instead of the color sensor because we identified candidate heat signatures in the infrared video before consulting color video. We estimated the standard error (SE) of $\hat{D}$ using an approach modified from the R2 method in Fewster et al. (2009), where

$$SE\,(\hat{D}) = \sqrt{\frac{J}{Q^2(J-1)} \sum_{j=1}^{J} q_j^2 \left(\frac{n_j}{q_j} - \frac{n}{Q}\right)^2} \tag{6}$$

and J = the number of transects, q_j = the total area sampled on transect j, and n_j = the total number of detections on transect j. We then propagated the error from the probability of detecting an infrared heat signature into $SE\,(\hat{D})$ using the delta method.

Comparing methods and cost-effectiveness analysis

We compared the performance of fecal-pellet, camera-trap, and aerial sampling along multiple dimensions associated with a single application of each field method in each RMU. These dimensions included the CV of the density estimate, the spatial extent of sampling, the initial cost required to attain an estimate, and the recurring costs for continued use. We compared the relative precision of each density estimate using the coefficient of variation (CV). For spatial extent we compared the total area, a, over which density was inferred by each method. Consistent with Laguardia et al. (2021), we defined a as the area of the sub-areas within each RMU for fecal-pellet and camera-trap sampling, and the area of the 41.44-km^2 areas in each RMU for aerial sampling. We assessed 3 measures of sampling costs: (1) capital, (2) field-operations, and (3) data-processing costs. The capital cost was defined as the annualized upfront expense for equipment. We did not consider the capital cost of field vehicles used for fecal-pellet and camera-trap sampling. In cases where we used the same field equipment for estimating density in each RMU for a particular method, the annualized upfront capital cost was divided between the 3 RMUs to calculate the cost per-use via the following formula:

$$CC_i = \frac{CC_I / A\,(r,N)}{U_I} * U_i \tag{7}$$

where CC_i = the repeated capital cost for the ith RMU, CC_I = the total cost of the repeatedly used capital across all I RMUs, U_I = the total usage (e.g., number of transects or points sampled with capital) of the repeatedly used capital across all I RMUs per application, and U_i = the usage of the repeatedly used capital for the ith RMU. In cases where select field operations were performed to conduct field work on all RMUs (e.g., installing sensors on the aircraft), this cost was divided between RMUs by removing the annuity factor and replacing capital cost with the cost of the select field operations in Equation 7. We decided to split shared costs between RMUs because the Indiana Department of Natural Resources requires density estimates across at least 3 RMUs per sampling year, and we suspect that other states may also require estimates for multiple areas. The field-operations cost was defined as the recurring cost associated with each field application of the method to estimate density. Lastly, we defined the data-processing cost as the cost to process the data which included the hourly cost of entering data, viewing and scoring aerial footage, classifying species within camera-trap photos, measuring distances to deer within camera-trap photos, and analysis.

We calculated the cost effectiveness of each method using Equations 1 and 2. We calculated annualized capital costs assuming $N = 1, 2..., 15$ applications to assess the sensitivity of our cost-effectiveness ratios to the lifespans of capital equipment. Lastly, we repeated these analyses while allowing for user-specified weights using Equation 3. We specified weights using the importance scores given by the Indiana state deer biologist. Specifically, we used the following importance scores: $i_{cv} = 100$, $i_{CC} = 10$, $i_{FOC} = 40$, $i_{DPC} = 20$, and $i_a = 100$, which corresponded to weights of $w_{cv} = 1.852$, $w_{CC} = 0.185$, $w_{FOC} = 0.741$, $w_{DPC} = 0.370$, and $w_a = 1.852$. We performed all analyses using the R programming language version 4.1.2 (R Core Team 2021).

RESULTS

Fecal pellet sampling

In total, we surveyed 263 transects covering 52.6 km and detected 1,262 fecal-pellet groups across all 3 RMUs. A stratified detection function across open and concealed habitats was most parsimonious when we fit candidate detection functions to cumulative data collected across all RMUs (ΔAIC = 872.1). Following this, a pooled detection function and stratified encounter rate were most parsimonious across the RMUs for both open (ΔAIC = 45.8) and concealed (ΔAIC = 476.6) habitats. Lastly, a pooled detection function and stratified encounter rate were most parsimonious across grassland and agriculture within open habitats (ΔAIC = 43.9). Thus, we used unique detection functions for open and concealed habitat, and a stratified encounter rate to estimate RMU-specific densities for each habitat type. We truncated all detections >110 cm and >150 cm from the transect line in open and concealed habitat, respectively, to remove a right tail of distances with low associated detection probabilities (Buckland et al. 2001). Truncation removed a total of 100 detections. Following truncation, the hazard-rate detection function with no adjustments or covariates (ΔAIC = 1.02, Cramer-von Mises GOF $P = 0.89$) and the half-normal detection function with observer and sub-area as covariates (ΔAIC = 2.5, Cramer-von Mises GOF $P = 0.21$) were the AIC-best models in open and concealed habitat types, respectively. In RMU 3, 4, and 9, we estimated $\hat{t}$ at 45.2 (SE = 3.1), 31.9 (SE = 5.4), and 51.9 (SE = 3.1) days in concealment, 71.5 (SE = 3.1), 53.7 (SE = 10.4), and 78.3 (SE = 3.5) days in agricultural fields, and 106.5 (SE = 3.9), 77.3 (SE = 8.4), and 111.6 (SE = 5.9) days in prairies, respectively.

The average density from fecal-pellet sampling across RMUs in open, concealed, and across both habitats was 6.48 (SE = 2.33), 15.20 (SE = 0.23), and 9.59 (SE = 1.89) deer/km^2, respectively. The average CV of density in open, concealed, and across both habitats was 0.50 (SE = 0.08), 0.20 (SE = 0.03), and 0.28 (SE = 0.02), respectively. Within each RMU, the densities in concealed habitat were always larger than those in open habitat (Table 1). Similarly, within each RMU, the CVs of densities in concealed habitat were always smaller than those in open habitat. The average capital, data-processing, and field-operations costs across RMUs was $427 (SE = $50), $116 (SE = $9) and $4,045 (SE = $396; Table 2), respectively. The total area for fecal-pellet sampling was 72.5 km^2 for both RMU 3 and 9, and 62.2 km^2 for RMU 4. The average cost effectiveness and weighted cost effectiveness across RMUs for fecal-pellet sampling was 18.27 (SE = 1.26) and 12.40 (SE = 0.87), respectively.

Camera-trap sampling

We deployed 428 camera traps and captured a total of 1,015,178 photos. We removed 21 camera traps from our analysis due to placement concerns (e.g., pointed downward or upward) resulting in 407 camera traps used to

TABLE 1 Density estimates of white-tailed deer from fecal-pellet data collected from 1–24 March 2021 in 3 different regional management units (RMU) of Indiana, USA. Densities and corresponding measures of precision were estimated using conventional distance sampling, and are shown for concealed, open, and across both concealed and open (Total) habitat types. The number of 200-m transects surveyed (k) and number of detections after truncation (n) are presented for each RMU and habitat type.

Habitat	RMU	k	n	$\hat{D}$	$SE(\hat{D})$	$CV(\hat{D})$
Concealed	3	42	246	14.919	2.694	0.181
Concealed	4	88	395	15.011	3.763	0.251
Concealed	9	46	298	15.661	2.506	0.16
Open	3	57	122	4.737	1.932	0.408
Open	4	9	9	3.607	2.393	0.663
Open	9	21	92	11.097	4.893	0.441
Total	3	99	368	5.922	1.736	0.293
Total	4	97	404	10.673	2.503	0.235
Total	9	67	390	12.189	3.771	0.309

TABLE 2 The capital (CC), field operation (FOC), and data processing costs (USD; DPC), area over which density was inferred (km^2), coefficient of variation (CV), cost effectiveness (CE), and weighted cost effectiveness (CE_w) associated with density estimates from fecal-pellet (PS), camera-trap (CS), and aerial (AS) sampling in regional management units (RMU) 3, 4, and 9 within Indiana, USA, in 2021. Weights were assigned by the Indiana state deer biologist. Capital costs were annualized across a single application. We underlined the best index within each RMU.

Method	RMU	CC	FOC	DPC	Area	CV	CE	CE_w
PS	3	482	4107	110	72	0.29	18.98	12.82
PS	4	472	4699	104	62	0.24	19.94	13.64
PS	9	326	3330	134	72	0.31	15.79	10.72
CS	3	19714	7986	3126	72	0.15	65.61	22.82
CS	4	15967	6156	2412	62	0.18	69.03	23.66
CS	9	19475	7330	5181	72	0.12	52.71	18.05
AS	3	28606	4260	729	290	0.17	19.34	5.02
AS	4	24520	3819	695	249	0.13	15.18	3.99
AS	9	28606	4362	723	290	0.11	12.19	3.18

estimate density (Table 3). We used data collected during a 2-week period from 25 February to 10 March 2021 in order to streamline data analysis. Within this 2-week period, we captured 294,335 photos, 81,740 of which contained deer. We measured a total of 30,732 and 9,505 distances in concealed and open habitat, respectively. During preliminary investigation of the data, we observed a spike in detections near camera traps in open habitat. Because of this, we did not consider the hazard-rate key function during model selection in open habitat, because this model can fit unnaturally large spikes at close distances resulting in an unnaturally abrupt decline in detectability as distance increases. After removing the hazard rate model from consideration in open habitat, we

TABLE 3 Density estimates of white-tailed deer from camera-trap sampling data collected from 25 February to 10 March 2021 in 3 different regional management units (RMU) of Indiana, USA. Densities and corresponding measures of precision were estimated using conventional distance sampling, and are shown for concealed, open, and across both concealed and open (Total) habitat types. The number of cameras deployed (k) and the number of detections after truncation (n) are presented for each RMU and habitat type.

Habitat	RMU	k	n	$\hat{D}$	$SE(\hat{D})$	$CV(\hat{D})$
Concealed	3	85	6,549	11.791	1.893	0.161
Concealed	4	91	4,642	6.600	1.223	0.185
Concealed	9	108	19,541	24.055	3.513	0.146
Open	3	60	2,459	3.806	0.789	0.207
Open	4	23	2,040	7.029	2.388	0.340
Open	9	40	5,006	10.642	1.875	0.176
Total	3	145	9,008	4.736	0.731	0.154
Total	4	114	6,682	6.763	1.183	0.175
Total	9	148	24,547	13.851	1.655	0.120

found a stratified detection function across open and concealed habitat to be most parsimonious (ΔQAIC = 1,298.2). We found the uniform key function with 1 cosine adjustment ($\Delta\chi^2/_{df}$ = 332.2) and the uniform key function with 2 cosine adjustment terms ($\Delta\chi^2/_{df}$ = 190.7) to be the best detection functions in open and concealed habitats, respectively. In RMU 3, 4, and 9, we estimated $\hat{A}$ at 0.38 (SE = 0.02), 0.43 (SE = 0.03), and 0.42 (SE = 0.01), respectively.

The average density from camera-trap sampling across RMUs in open, concealed, and across both habitats was 7.16 (SE = 1.97), 14.15 (SE = 5.17), and 8.45 (SE = 2.76) deer/km^2, respectively. The average CV of density in open, concealed, and across both habitats was 0.24 (SE = 0.05), 0.16 (SE = 0.01), and 0.15 (SE = 0.02), respectively. Density estimates in concealed habitat were larger than those in open habitat in RMU 3 and 9, but the reverse was true for RMU 4 (Table 3). The CVs of densities in concealed habitat were always smaller than those in open habitat. Similar to fecal-pellet sampling, total density was largest for RMU 9 and smallest for RMU 3. The average capital, data-processing, and field-operations costs across RMUs was $18,385 (SE = $1,211), $3,573 (SE = $830), and $7,157 (SE = $535; Table 2), respectively. The total area for camera-trap sampling was 72.5 km^2 each for RMUs 3 and 9, and 62.2 km^2 for RMU 4. The average cost effectiveness and weighted cost effectiveness across RMUs for camera-trap sampling was 62.45 (SE = 4.97) and 21.51 (SE = 1.75), respectively.

Aerial sampling

We recorded video on 111, 96, and 112 transects in RMUs 3, 4, and 9, respectively. On a single transect in RMU 3, our video recording system failed to record, which resulted in 111 transect videos instead of 112. We recorded 6.90, 5.49, and 6.67 hours of video in RMUs 3, 4, and 9, respectively.

The average density from aerial sampling across RMUs in open, concealed, and across both habitats was 1.31 (SE = 0.49), 21.64 (SE = 7.95), and 6.11 (SE = 2.06) deer/km^2, respectively. The average CV of density in open, concealed, and across both habitats was 0.36 (SE = 0.01), 0.14 (SE = 0.02), and 0.13 (SE = 0.02), respectively. Within each RMU, the densities in concealed habitat were always larger than those in open habitat (Table 4). Similarly, within each RMU, the CVs of densities in concealed habitat were always smaller than those in open habitat. The average capital, data-processing, and field-operations costs across RMUs was $27,244 (SE = $1,362), $716

TABLE 4 Density estimates of white-tailed deer from aerial-sampling data collected from 8 February to 10 March 2021 in 3 different regional management units (RMU) of Indiana, USA. Densities and corresponding measures of precision were estimated using plot sampling methods, and are shown for concealed, open, and across both concealed and open (Total) habitat types. The area captured by the field-of-view of the vertical-looking infrared thermographer (Q), as well as the number of detections after truncation (n) are presented for each RMU and habitat type.

Habitat	RMU	Q	n	$\hat{D}$	$SE(\hat{D})$	$CV(\hat{D})$
Concealed	3	13.8	250	22.349	4.074	0.182
Concealed	4	50.34	379	7.528	1.036	0.138
Concealed	9	20.54	671	35.038	3.662	0.105
Open	3	76.35	42	0.679	0.247	0.363
Open	4	22.55	22	0.976	0.362	0.371
Open	9	39.29	83	2.266	0.773	0.341
Total	3	90.15	292	3.202	0.534	0.167
Total	4	72.89	401	5.035	0.657	0.13
Total	9	59.83	754	10.105	1.063	0.105

(SE = \$10) and \$4,147 (SE = \$167; Table 2), respectively. The total area for aerial sampling was 290.1 km^2 each for RMUs 3 and 9, and 248.6 km^2 for RMU 4. The average cost effectiveness and weighted cost effectiveness across RMUs for aerial sampling was 15.83 (SE = 2.11) and 4.11 (SE = 0.54), respectively.

Comparing methods and cost-effectiveness analysis

Total density estimates from aerial sampling were consistently smaller than density estimates from the other methods. All 3 methods suggested that total densities of deer were largest in RMU 9 and smallest in RMU 3. Aerial and camera-trap sampling always had the lowest CVs. The lowest capital, field-operating, and data-processing costs were associated with fecal-pellet sampling, except field-operating costs for aerial sampling in RMU 4 (Tables 2 and 5).

After a single application (i.e., capital costs annualized across a single application), aerial sampling was the most cost effective in RMUs 4 and 9, while fecal-pellet sampling was the most cost effective in RMU 3 (Table 2). However, when differential weights were used with input parameters, aerial sampling was always the most cost-effective method after a single application of each method. When annualizing the capital costs of each method across 1, 2…,15 applications, the cost effectiveness of aerial sampling improved with increasing number of applications at a more rapid rate than that of fecal-pellet sampling. Although cost effectiveness of camera-trap sampling was most sensitive to the number of applications, camera-trap sampling still never surpassed either fecal-pellet or aerial sampling, regardless of whether differential weights were used or how many applications capital cost was annualized across (Figure 2).

DISCUSSION

Cost-effectiveness analysis is a simple and powerful tool to decide between competing methods to estimate animal density. Past evaluations of methods used for estimating animal densities usually compared the cost and various factors related to the performance of methods separately (Anderson et al. 2013, Hedges et al. 2013,

TABLE 5 A breakdown of cost (USD) sources comprising capital (CC), field-operating (FOC), and data-processing (DPC) costs for aerial, camera-trap, and fecal-pellet sampling methods used to estimate white-tailed deer density in Indiana, USA. Deer densities were estimated in Deer Regional Management Units (RMU) 3, 4, and 9. Costs per unit, hour of operation, or mile (Cost/UHM) and the number of units, hours of operation, or miles (No. of UHM) for each source of cost are presented.

Method	Type	Source	Cost/UHM	No. of UHM	RMU 3	RMU 4	RMU 9
Pellet	CC	Field equipment	272.13	Variable[a]	468	458	317
	FOC	Field labor	17.76	534	3,229	3,894	2,362
		Travel (gas)	0.58	892	161	189	168
		Study design labor	26.39	18	166	143	166
		Land permission	1,575.00	NA	551	473	551
	DPC	Analysis labor	24.38	14	110	104	134
Camera	CC	Camera equipment[b]	119.02	428	18,210	14,758	17,972
		Field equipment[c]	272.13	4	388	305	396
		Equipment shipping	1,520.00	1	542	438	540
	FOC	Field labor[d]	18.35	784	5,515	4,007	4,866
		Travel (gas)	0.58	1,784	321	379	335
		Study design labor	26.39	7	65	55	65
		Batteries	1.67	2,568	1,533	1,242	1,513
		Land permission	1,575.00	NA	551	473	551
	DPC	Downloading labor	24.38	40	349	283	344
		Classification labor[e]	14.40	169	870	557	1,008
		Distance labor	13.79	424	1,420	1,086	3,342
		Analysis labor	24.38	60	488	488	488
Aerial	CC	IR sensor	33,488.00	1	11,721	10,046	11,721
		Color sensor	4,088.90	1	1,431	1,227	1,431
		Pod engineering	95.00	209	6,949	5,957	6,949
		GeoDVR[f]	18,510.00	1	6,479	5,553	6,479
		Equipment shipping	3,410.25	1	1,194	1,023	1,194
	FOC	Plane usage	237.00	37	2,989	2,714	3,081
		Operational labor	24.38	37	307	279	317
		Study design labor	26.39	9	83	71	83
		Sensor installation	95.00	18	599	513	599
		Sensor removal	95.00	9	283	242	283
	DPC	Viewing labor	24.38	28	241	207	236
		Analysis labor	24.38	60	488	488	488

[a]Field equipment for pellet sampling included 8 tape measures and 4 GPS units.

[b]Camera equipment includes the cost of cameras, security boxes, python cables, and SD cards.

[c]Field equipment includes the cost of compasses, tape measures, and GPS units.

[d]Field labor cost/hour is a weighted average (weighted based on hours of labor) between coordinator ($25.58 USD/hour), technician ($13.32 USD/hour), and graduate student ($24.38 USD/hour) labor.

[e]Classification labor is a weighted average (weighted based on hours of labor) between technician ($13.32 USD/hour) and graduate student ($24.38 USD/hour) labor.

[f]GeoDVR includes the price of the GeoDVR as well as upgrades and accessories that we required.

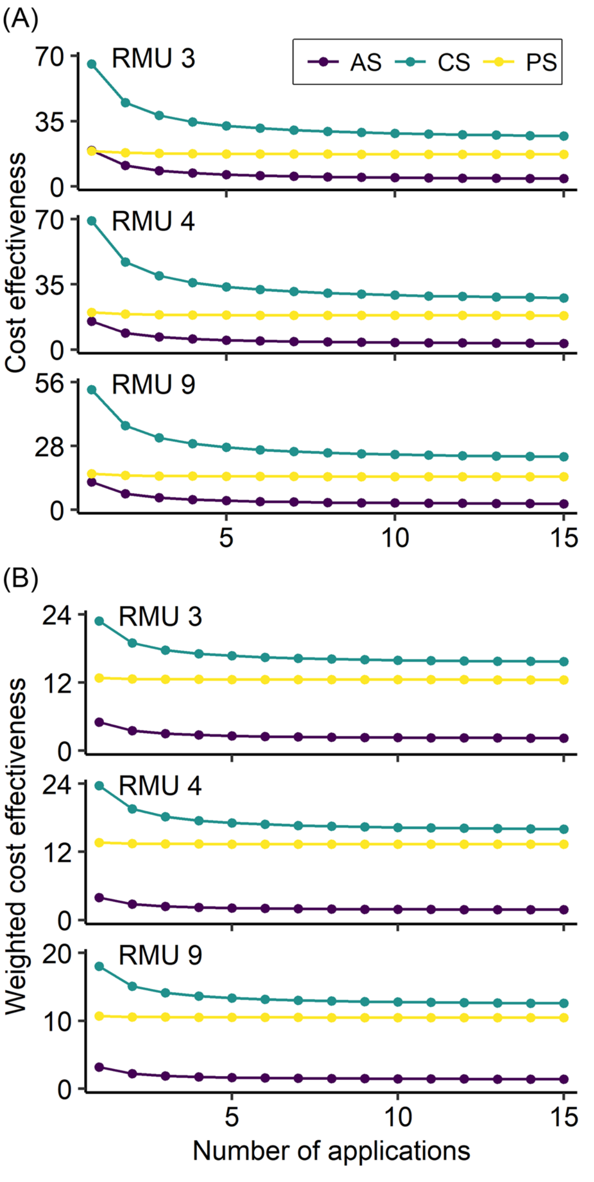

FIGURE 2 The cost-effectiveness (a) and weighted cost-effectiveness (b) of aerial (AS), camera-trap (CS), and fecal-pellet sampling (PS) when estimating the density of white-tailed deer in Regional Management Units (RMU) 3, 4, and 9 within Indiana, USA, in 2021. Capital cost was annualized across 1, 2..., 15-application lifespans.

Zero et al. 2013). Unfortunately, such comparisons can lead to conflicting results that can confound decision makers (e.g., one method is more precise, but another requires less money). Therefore, we developed a cost-effectiveness model that integrates cost, performance, and scale into a single, comparable, and easily interpretable value (e.g., cost per unit land area standardized by relative precision) for methods estimating density.

Wildlife management agencies are limited by funding (Leopold et al. 2018), and thus decisions about the cost effectiveness of a management technique should affect the selection and quantity of management activities in which managers engage (Anderson and Loomis 2006). However, whether a method can actually be implemented (i.e., feasibility; Hopfensperger et al. 2007, Bowen et al. 2009) may depend on factors other than those included in cost-effectiveness analysis. Laguardia et al. (2021) introduced a metric they termed an integrated feasibility index which incorporated similar parameters as our model (cost, scale, and precision), but their index does not assess feasibility. Indeed, simple rearrangement reveals that their index is a modified cost-effectiveness ratio of the form given in Equation 1. More appropriately, factors that determine feasibility are a result of constraints placed on an agency by internal or external forces. Internal constraints may be related to operational priorities, which limit the amount of money that can be spent on a project or the number of personnel assigned to the task. External constraints are often beyond the control of natural resource agencies and may include bureaucratic restrictions such as limits on the maximum number of personnel allowed for hiring, or the maximum number of vehicles allowed for purchasing, regardless of whether the agency can afford more personnel or vehicles. External constraints may limit feasibility even when internal constraints are absent. Therefore, agencies must identify the factors affecting the feasibility of a method before consideration and adjust how methods are applied to ensure feasibility prior to assessing cost effectiveness.

Due to limited funding, wildlife agencies may be more inclined to spend funds on methods that have the potential to collect additional biological information in conjunction with the target data. When using our study-design methods, camera-trap sampling can also be used to estimate the density or occurrence of many other species captured in images, and can answer other questions related to behavior, health, and demographics (Delisle et al. 2021). Aerial sampling using infrared thermographers can estimate the density of other medium to large endotherms (Chrétien et al. 2015). When conducting field work for fecal-pellet sampling, fecal pellets may be simultaneously collected for genetic analyses (Kaunisto et al. 2017), or other animal sign recorded (Wood 1988). Similar to feasibility constraints, the value put on the potential to collect additional information depends on management objectives and funding; therefore, we did not explicitly consider the potential to collect additional information. If agencies do consider the additive utility of competing methods, then the added utility should be discounted appropriately according to its value relative to the importance of the primary purpose of the survey.

We used aerial, fecal-pellet, and camera-trap sampling to estimate the density of a common ungulate in 3 large regions. Based on weighted and non-weighted cost-effectiveness analysis, aerial sampling was the most cost effective when annualizing the capital cost of each method across multiple applications. Aside from annualizing capital costs across only a single application, the superior cost effectiveness of aerial sampling was apparent in all 3 RMUs, which suggests consistency even for landscapes with vastly different habitat compositions and varying densities. These findings are dependent on our method which splits the shared costs across RMUs. We decided to split shared costs between RMUs because future management objectives of the Indiana Department of Natural Resources seek to estimate deer density (1) in the remaining RMUs within the state, (2) across no fewer than 3 RMUs per sampling year, and (3) repetitively across many future sampling years. The RMUs included in the current study span the range of landscape conditions in the state, and thus we believe the better long-term cost effectiveness of aerial sampling will hold true in the remaining RMUs. More generally, we suspect that the superior long-term cost effectiveness of aerial sampling will translate to density estimation of other common endothermic species that can be detected using infrared thermographers in similarly sized or larger areas outside of Indiana.

A substantial portion of our field operating costs for camera-trap and fecal-pellet sampling were associated with acquiring permission to sample on private property. Aerial sampling forgoes this requirement, as airspace is not privately owned. We predict narrower differences between the cost-effectiveness ratios of aerial sampling and fecal-pellet and camera-trap sampling for studies similar to ours but conducted in areas dominated by public lands. In comparison to the other methods we considered, camera-trap sampling had higher field-operation and data-processing costs (i.e., recurring costs). Specifically, the mean data processing costs for camera-trap sampling per RMU were \$30.1 (SE = \$4.5) and \$5.0 (SE = \$1.1) USD times greater than those from fecal-pellet and aerial sampling, respectively. Such discrepancies might discourage future researchers from using camera traps to estimate trends in density across large spatiotemporal expanses, but this finding reflects the current technology available for accurately processing data. Models for automated species tagging (Willi et al. 2019, Norouzzadeh et al. 2021) and distance estimation (Haucke et al. 2021, Zuleger et al. 2022) appear promising and, if easy-to-use forms are readily available in the future, could substantially decrease the cost of processing data from camera traps. To predict future cost effectiveness, we simulated a reduction in the data-processing cost of camera-trap sampling to $200; however, the weighted and unweighted cost-effectiveness ratios showed the same preference rankings across methods. Therefore, despite the increased usage of camera traps (Delisle et al. 2021), our study suggests the cost effectiveness of camera-trap sampling for estimating density across larger heterogenous landscapes is poor in comparison to alternative methods.

Within each RMU, densities from aerial sampling in open and concealed habitats were considerably lower and higher (except in RMU 4), respectively, than the other 2 methods. These patterns likely resulted because we conducted aerial sampling diurnally when deer were less likely to use open habitats (Larson et al. 1978). Our density estimates from camera traps and pellet counts both incorporated nighttime hours when deer are far more likely to use open habitat types (Larson et al. 1978). Specifically, density estimates from pellet sampling represent an average density across the time it takes pellet groups to decay (Marques et al. 2001), and densities from camera sampling are an average density across the snapshot moments during the time cameras are sampling. Therefore, interpretation of differences between density estimates from the 3 methods should focus on the total density across both open and concealed habitat types.

Density estimates from aerial and camera-trap sampling had lower CVs than the estimates from pellet sampling. Uncertainty from many different sources can impact the variation of density estimates (Williams et al. 2002). These sources of variation include detectability as a function of distance (Buckland et al. 2001), observer (Buckland and Garthwaite 1991), or a combination of these and other covariates (Burt et al. 2014); multipliers such as activity or availability levels (Howe et al. 2017), group size (Hamilton et al. 2018), and persistence or production of cues (Marques et al. 2001, Buckland et al. 2008); classification discrepancies among observers (Delisle et al. 2022*b*); and the encounter rate between transects or points (Fewster et al. 2009). Our estimates from aerial sampling only addressed variation from the encounter rate and detectability differences between viewers of infrared video. Similarly, the estimates from camera trapping and pellet sampling addressed variation from the encounter rate, detection function, and multipliers (activity level and dung persistence rate), but spatial replicates were more plentiful for camera trapping. These additional sources of variation and fewer spatial replicates likely contributed to the higher CVs of density estimates from pellet sampling.

Although we used 3 common field-sampling methods under, perhaps, the most common statistical estimator used for estimating wildlife density (distance sampling), other sampling methods and estimators exist. Field-sampling methods related to density estimation that we did not consider include, but are not limited to, drones (Chrétien et al. 2016) and spotlighting (McCullough 1982). Similarly, other statistical estimators of density include, but are not limited to, capture-recapture methods (Royle et al. 2013), N-mixture models (Royle 2004), and random encounter or random encounter and staying time models (Rowcliffe et al. 2008, Nakashima et al. 2018). We chose to implement fecal-pellet, camera-trapping, and aerial sampling methods under a distance-sampling framework because these strategies could be reasonably applied while meeting study-design and sampling assumptions. Even subtle changes to field sampling and statistical methods could alter costs or precision. For instance, guidelines with case studies are needed on how best to account for factors such as reactive behavior toward cameras. We encourage future comparisons of the cost effectiveness of other field sampling and statistical methods, and how cost effectiveness is influenced by finer examination of other field-sampling and statistical decisions within common density estimators.

We extended cost-effectiveness analysis to specifically decide between density-estimation methods, and we believe that the same principles can be used to decide between competing alternatives related to many types of ecological monitoring. For example, several methods exist that aim to reduce human-wildlife conflict (Tarlow and Blumstein 2007) or measure the impacts of herbivores on plant communities (Kirschbaum and Anacker 2005, Royo et al. 2016). Simple alterations to our cost-effectiveness analysis can aid these decisions. Similarly, methods that integrate multiple data types to produce a single estimate (i.e., fusion models) are becoming more popular due to increased precision (Zipkin et al. 2021). Our approach to cost-effectiveness analysis offers a formal framework to determine whether the improved precision is worth the extra cost and effort to collect multiple data types.

MANAGEMENT IMPLICATIONS

When considering the cost effectiveness of field methods, the relative importance of cost, precision, and area sampled depends on context, and each agency will have its own set of parameters with which to contend (Leopold et al. 2018). Unfortunately, most cost-effectiveness analyses do not take this into consideration. When we used equal weights of importance for input parameters, the cost-effectiveness ratios of aerial and fecal-pellet sampling were very similar after a single application of each method. However, because the deer manager in Indiana allocated low importance to cost-related parameters and placed much greater value on the precision of the density estimate, aerial sampling was clearly identified as the most cost-effective approach. In general, wildlife managers should use our weighted cost-effectiveness ratio (Equation 3), because it permits users to specify importance of each parameter and thus flexibly accommodates the unique context faced by each agency. Context-independent comparisons of methods across agencies or jurisdictions should use cost-effectiveness ratios computed using Equations 1 and 2.

ACKNOWLEDGMENTS

We thank the 266 private property owners that allowed us to conduct research on their properties, L. Utley for GIS assistance, R. Sample for support writing descriptions of the study area, S. Allaire for help with field-work coordination, several technicians that assisted with field work, and B. Stirm for installing the aerial-sampling equipment onto the aircraft. We appreciate helpful comments from 2 anonymous reviewers, E. Flaherty, and P. Zollner on this work. We gratefully acknowledge the traditional homelands of the Indigenous People upon which Purdue University is built and our fieldwork was conducted. We honor and appreciate the Bodéwadmik (Potawatomi), Lenape (Delaware), Myaamia (Miami), and Shawnee People who are the original Indigenous caretakers. This paper is a contribution of the Integrated Deer Management Project, a collaborative research effort between Purdue University and the Indiana Department of Natural Resources Division of Fish and Wildlife. Funding was provided by the Indiana Department of Natural Resources Grant W-48-R-02.

CONFLICTS OF INTEREST STATEMENT

The authors declare no conflicts of interest.

DATA AVAILABILITY STATEMENT

The data that support the findings of this study are available from the corresponding author upon reasonable request.

ETHICS STATEMENT

Our study did not involve live animal subjects. No permits or permissions were required for the research reported here.

ORCID

Zackary J. Delisle http://orcid.org/0000-0002-1942-7886
Patrick G. McGovern http://orcid.org/0000-0002-4433-4948
Robert K. Swihart http://orcid.org/0000-0002-4064-1940

REFERENCES

Anderson, L. E., and D. K. Loomis. 2006. Balancing stakeholders with an imbalanced budget: how continued inequities in wildlife funding maintains old management styles. Human Dimensions of Wildlife 11:455–458.

Anderson, C. W., C. K. Nielsen, C. M. Hester, R. D. Hubbard, J. K. Stroud, and E. M. Schauber. 2013. Comparison of indirect and direct methods of distance sampling for estimating density of white-tailed deer. Wildlife Society Bulletin 37: 146–154.

Anile, S., B. Ragni, E. Randi, F. Mattucci, and F. Rovero. 2014. Wildcat population density on the Etna volcano, Italy: a comparison of density estimation methods. Journal of Zoology 293:252–261.

Barnes, R. F. 2001. How reliable are dung counts for estimating elephant numbers? African Journal of Ecology 39:1–9.

Beier, P., and D. R. McCullough. 1990. Factors influencing white-tailed deer activity patterns and habitat use. Wildlife Monographs 109:1–51.

Bernatas, S., and L. Nelson. 2004. Sightability model for California bighorn sheep in canyonlands using forward-looking infrared (FLIR). Wildlife Society Bulletin 32:638–647.

Boardman, A. E., D. H. Greenberg, A. R. Vining, and D. L. Weimer. 2011. Pages 464–473 *in* A. E. Boardman, D. H. Greenberg, A. R. Vining, and D. L. Weimer, editors. Cost-benefit analysis: concepts and practice. Prentice Hall Publishers, Upper Saddle River, New Jersey, USA.

Bowen, D. J., M. Kreuter, B. Spring, L. Cofta-Woerpel, L. Linnan, D. Weiner, S. Bakken, C. P. Kaplan, L. Squiers, C. Fabrizio, et al. 2009. How we design feasibility studies. American Journal of Preventive Medicine 36:452–457.

Brack, I. V., A. Kindel, and L. F. B. Oliveira. 2018. Detection errors in wildlife abundance estimates from Unmanned Aerial Systems (UAS) surveys: Synthesis, solutions, and challenges. Methods in Ecology and Evolution 9:1864–1873.

Buckland, S. T., D. R. Anderson, K. P. Burnham, J. L. Laake, D. L. Borchers, and L. Thomas. 2001. Introduction to distance sampling: estimating abundance of biological populations. Oxford University Press, Oxford, UK.

Buckland, S. T., and P. H. Garthwaite. 1991. Quantifying precision of mark-recapture estimates using the bootstrap and related methods. Biometrics 47:255–268.

Buckland, S. T., S. J. Marsden, and R. E. Green. 2008. Estimating bird abundance: Making methods work. Bird Conservation International 18:S91–S108.

Buckland, S. T., E. A. Rexstad, T. A. Marques, and C. S. Oedekoven. 2015. Distance sampling: methods and applications. Springer, Heidelberg, Germany.

Burt, M. L., D. L. Borchers, K. J. Jenkins, and T. A. Marques. 2014. Using mark–recapture distance sampling methods on line transect surveys. Methods in Ecology and Evolution 5:1180–1191.

Campbell, H. F., and R. P. C. Brown. 2016. Project Appraisal and Principles. Pages 19–39 *in* H. F. Campbell and R. P. C. Brown, editors. Cost-Benefit Analysis: Financial and Economic Appraisal using Spreadsheets. Routledge, London, UK

Campbell, D., G. M. Swanson, and J. Sales. 2004. Methodological insights: comparing the precision and cost-effectiveness of faecal pellet group count methods. Journal of Applied Ecology 41:1185–1196.

Caughley, G., and D. Grice. 1982. A correction factor for counting emus from the air, and its application to counts in Western Australia. Wildlife Research 9:253–259.

Chrétien, L. P., J. Théau, and P. Ménard. 2015. Wildlife multispecies remote sensing using visible and thermal infrared imagery acquired from an unmanned aerial vehicle (UAV). Proceedings of the International Conference on Unmanned Aerial Vehicles in Geomatics, Toronto, Canada. International Archives of the Photogrammetry, Remote Sensing and Spatial Information Sciences XL-1/W4:241–248.

Chrétien, L. P., J. Théau, and P. Ménard. 2016. Visible and thermal infrared remote sensing for the detection of white-tailed deer using an unmanned aerial system. Wildlife Society Bulletin 40:181–191.

Conover, M. R. 2001. Resolving human-wildlife conflicts: the science of wildlife damage management. CRC Press, Boca Raton, Florida, USA.

De Bondi, N., J. G. White, M. Stevens, and R. Cooke. 2010. A comparison of the effectiveness of camera trapping and live trapping for sampling terrestrial small-mammal communities. Wildlife Research 37:456–465.

Delisle, Z. J., E. A. Flaherty, M. R. Nobbe, C. M. Wzientek, and R. K. Swihart. 2021. Next-generation camera trapping: systematic review of historic trends suggests keys to expanded research applications in ecology and conservation. Frontiers in Ecology and Evolution 9:97.

Delisle, Z. J., P. G. McGovern, B. G. Dillman, and R. K. Swihart. 2022*a*. Imperfect detection and wildlife density estimation using aerial surveys with infrared and visible sensors. Remote Sensing in Ecology and Conservation. Early View. https://doi.org/10.1002/rse2.305

Delisle, Z. J., R. K. Swihart, B. M. Quinby, R. D. Sample, K. J. Kinser-McBee, E. K. Tauber, and E. A. Flaherty. 2022*b*. Density from pellet groups: comparing methods for estimating dung persistence time. Wildlife Society Bulletin 46(3):e1325.

Devers, P. K., R. L. Emmet, G. S. Boomer, G. S. Zimmerman, and J. A. Royle. 2021. Evaluation of a 2-season banding program to estimate and model migratory bird survival. Ecological Applications 31(7):e02425.

Fewster, R. M., S. T. Buckland, K. P. Burnham, D. L. Borchers, P. E. Jupp, J. L. Laake, and L. Thomas. 2009. Estimating the encounter rate variance in distance sampling. Biometrics 65:225–236.

Fleming, P. J., and J. P. Tracey. 2008. Some human, aircraft and animal factors affecting aerial surveys: how to enumerate animals from the air. Wildlife Research 35:258–267.

Franke, U., B. Goll, U. Hohmann, and M. Heurich. 2012. Aerial ungulate surveys with a combination of infrared and high – resolution natural color images. Animal Biodiversity and Conservation 35:285–293.

Glover-Kapfer, P., C. A. Soto-Navarro, and O. R. Wearn. 2019. Camera-trapping version 3.0: current constraints and future priorities for development. Remote Sensing in Ecology and Conservation 5:209–223.

Hamilton, O. N., S. E. Kincaid, R. Constantine, L. Kozmian-Ledward, C. G. Walker, and R. M. Fewster. 2018. Accounting for uncertainty in duplicate identification and group size judgements in mark–recapture distance sampling. Methods in Ecology and Evolution 9:354–362.

Haucke, T., H. S. Kühl, J. Hoyer, and V. Steinhage. 2021. Overcoming the distance estimation bottleneck in estimating animal abundance with camera traps. Ecological Informatics 68:101536.

Haufler, J. B., S. R. Winterstein, and L. C. Bender. 1993. An aerial censusing procedure for elk in Michigan. Wildlife Society Bulletin 21:73–80.

Hawkins, C. E., and P. A. Racey. 2005. Low population density of a tropical forest carnivore, *Cryptoprocta ferox*: implications for protected area management. Oryx 39:35–43.

Hedges, S., A. Johnson, M. Ahlering, M. Tyson, and L. S. Eggert. 2013. Accuracy, precision, and cost-effectiveness of conventional dung density and fecal DNA based survey methods to estimate Asian elephant (*Elephas maximus*) population size and structure. Biological Conservation 159:101–108.

Hopfensperger, K. N., K. A. Engelhardt, and S. W. Seagle. 2007. Ecological feasibility studies in restoration decision making. Environmental Management 39:843–852.

Howe, E. J., S. T. Buckland, M. L. Després-Einspenner, and H. S. Kühl. 2017. Distance sampling with camera traps. Methods in Ecology and Evolution 8:1558–1565.

Howe, E. J., S. T. Buckland, M. L. Després-Einspenner, and H. S. Kühl. 2019. Model selection with overdispersed distance sampling data. Methods in Ecology and Evolution 10:38–47.

Hussain, A., J. B. Armstrong, D. B. Brown, and J. Hogland. 2007. Land-use pattern, urbanization, and deer–vehicle collisions in Alabama. Human-Wildlife Conflicts 1:89–96.

Jachmann, H. 2002. Comparison of aerial counts with ground counts for large African herbivores. Journal of Applied Ecology 39:841–852.

Kaunisto, K. M., T. Roslin, I. E. Sääksjärvi, and E. J. Vesterinen. 2017. Pellets of proof: First glimpse of the dietary composition of adult odonates as revealed by metabarcoding of feces. Ecology and Evolution 7:8588–8598.

Keiter, D. A., A. J. Davis, O. E. Rhodes, F. L. Cunningham, J. C. Kilgo, K. M. Pepin, and J. C. Beasley. 2017. Effects of scale of movement, detection probability, and true population density on common methods of estimating population density. Scientific Reports 7:1–12.

Kirschbaum, C. D., and B. L. Anacker. 2005. The utility of *Trillium* and *Maianthemum* as phyto-indicators of deer impact in northwestern Pennsylvania, USA. Forest Ecology and Management 217:54–66.

Kissell, R. E., and S. K. Nimmo. 2011. A technique to estimate white-tailed deer *Odocoileus virginianus* density using vertical-looking infrared imagery. Wildlife Biology 17:85–92.

Laake, J., M. J. Dawson, and J. Hone. 2008. Visibility bias in aerial survey: mark–recapture, line-transect or both? Wildlife Research 35:299–309.

Laguardia, A., K. S. Gobush, S. Bourgeois, S. Strindberg, G. Abitsi, F. Ebouta, J. M. Fay, A. M. Gopalaswamy, F. Maisels, R. Ogden, et al. 2021. Assessing the feasibility of density estimation methodologies for African forest elephant at large spatial scales. Global Ecology and Conservation 27(2021):e01550.

Larson, T. J., O. J. Rongstad, and F. W. Terbilcox. 1978. Movement and habitat use of white-tailed deer in southcentral Wisconsin. The Journal of Wildlife Management 42:113–117.

Leopold, B. D., W. B. Kessler, and J. L. Cummins. 2018. North American wildlife policy and law. Boone & Crockett Club, Missoula, Montana, USA.

Lewis, J. S., K. A. Logan, M. W. Alldredge, L. L. Bailey, S. VandeWoude, and K. R. Crooks. 2015. The effects of urbanization on population density, occupancy, and detection probability of wild felids. Ecological Applications 25:1880–1895.

Lyra-Jorge, M. C., G. Ciocheti, V. R. Pivello, and S. T. Meirelles. 2008. Comparing methods for sampling large-and medium-sized mammals: camera traps and track plots. European Journal of Wildlife Research 54:739–744.

Marques, F. F., S. T. Buckland, D. Goffin, C. E. Dixon, D. L. Borchers, B. A. Mayle, and A. J. Peace. 2001. Estimating deer abundance from line transect surveys of dung: sika deer in southern Scotland. Journal of Applied Ecology 38: 349–363.

McCullough, D. R. 1982. Evaluation of night spotlighting as a deer study technique. The Journal of Wildlife Management 46:963–973.

Meylan, A. B., and M. Donnelly. 1999. Status justification for listing the hawksbill turtle (*Eretmochelys imbricata*) as critically endangered on the 1996 IUCN Red List of Threatened Animals. Chelonian Conservation and Biology 3:200–224.

Miller, D. L. 2021. R Package 'Distance': Distance sampling detection function and abundance estimation. Version 1.0.4. https://cran.r-project.org/web/packages/Distance/Distance.pdf

Nakashima, Y., K. Fukasawa, and H. Samejima. 2018. Estimating animal density without individual recognition using information derivable exclusively from camera traps. Journal of Applied Ecology 55:735–744.

Nixon, C. M., L. P. Hansen, P. A. Brewer, and J. E. Chelsvig. 1991. Ecology of white-tailed deer in an intensively farmed region of Illinois. Wildlife Monographs 1:3–77.

Norouzzadeh, M. S., D. Morris, S. Beery, N. Joshi, N. Jojic, and J. Clune. 2021. A deep active learning system for species identification and counting in camera trap images. Methods in Ecology and Evolution 12:150–161.

Office of Management and Budget. 2003. Circular A-4. Executive order 12866. Washington D.C., USA.

Palencia, P., J. M. Rowcliffe, J. Vicente, and P. Acevedo. 2021. Assessing the camera trap methodologies used to estimate density of unmarked populations. Journal of Applied Ecology 58:1583–1592.

Parmenter, R. R., T. L. Yates, D. R. Anderson, K. P. Burnham, J. L. Dunnum, A. B. Franklin, M. T. Friggens, B. C. Lubow, M. Miller, G. S. Olson, et al. 2003. Small-mammal density estimation: a field comparison of grid-based vs. web-based density estimators. Ecological Monographs 73:1–26.

Péron, G., C. A. Nicolai, and D. N. Koons. 2012. Demographic response to perturbations: the role of compensatory density dependence in a North American duck under variable harvest regulations and changing habitat. Journal of Animal Ecology 81:960–969.

R Core Team. 2021. R: a language and environment for statistical computing. R Foundation for Statistical Computing, Vienna, Austria.

Rowcliffe, J. M. 2021. R Package 'activity': Animal activity statistics. Version 1.3.1. https://cran.r-project.org/web/packages/activity/activity.pdf

Rowcliffe, J. M., J. Field, S. T. Turvey, and C. Carbone. 2008. Estimating animal density using camera traps without the need for individual recognition. Journal of Applied Ecology 45:1228–1236.

Rowcliffe, J. M., R. Kays, B. Kranstauber, C. Carbone, and P. A. Jansen. 2014. Quantifying levels of animal activity using camera trap data. Methods in Ecology and Evolution 5:1170–1179.

Royle, J. A. 2004. N-mixture models for estimating population size from spatially replicated counts. Biometrics 60:108–115.

Royle, J. A., R. B. Chandler, R. Sollman, and B. Gardner. 2013. Spatial capture recapture. Elsevier, Oxford, United Kingdom.

Royo, A. A., D. W. Kramer, K. V. Miller, N. P. Nibbelink, and S. L. Stout. 2016. The canary in the coal mine: sprouts as a rapid indicator of browse impact in managed forests. Ecological Indicators 69:269–275.

Schaub, M, and M. Kéry. 2021. Integrated population models. Theory and ecological applications with R and JAGS. Academic Press, Cambridge, Massachusetts, USA.

Sinclair, A. R. 1991. Science and the practice of wildlife management. The Journal of Wildlife Management 55:767–773.

Skalski J. R., K. E. Ryding, and J. Millspaugh. 2005. Wildlife demography: analysis of sex, age, and count data. Elsevier Academic Press, Burlington, Massachusetts, USA.

Smith, T. S., S. C. Amstrup, B. J. Kirschhoffer, and G. York. 2020. Efficacy of aerial forward-looking infrared surveys for detecting polar bear maternal dens. PloS ONE 15(2):e0222744.

Spake, R., C. Bellamy, R. Gill, K. Watts, T. Wilson, B. Ditchburn, and F. Eigenbrod. 2020. Forest damage by deer depends on cross-scale interactions between climate, deer density and landscape structure. Journal of Applied Ecology 57: 1376–1390.

Stapleton, S., E. Peacock, and D. Garshelis. 2016. Aerial surveys suggest long-term stability in the seasonally ice-free Foxe Basin (Nunavut) polar bear population. Marine Mammal Science 32:181–201.

Storm, D. J., M. D. Samuel, T. R. Van Deelen, K. D. Malcolm, R. E. Rolley, N. A. Frost, D. P. Bates, and B. J. Richards. 2011. Comparison of visual-based helicopter and fixed-wing forward-looking infrared surveys for counting white-tailed deer *Odocoileus virginianus*. Wildlife Biology 17:431–440.

Swihart, R. K., J. N. Caudell, J. M. Brooke, and Z. Ma. 2020. A flexible model-based approach to delineate wildlife management units. Wildlife Society Bulletin 44:77–85.

Tarlow, E. M., and D. T. Blumstein. 2007. Evaluating methods to quantify anthropogenic stressors on wild animals. Applied Animal Behaviour Science 102:429–451.

Thiemann, G. W., A. E. Derocher, and I. Stirling. 2008. Polar bear *Ursus maritimus* conservation in Canada: an ecological basis for identifying designatable units. Oryx 42:504–515.

Todd, A. F., H. S. Kuehl, C. Cipolletta, and P. D. Walsh. 2008. Using dung to estimate gorilla density: modeling dung production rate. International Journal of Primatology 29:549–563.

Tombre, I. M., F. Fredriksen, O. Jerpstad, J. E. Østnes, and E. Eythórsson. 2022. Population control by means of organised hunting effort: Experiences from a voluntary goose hunting arrangement. Ambio 51:1–15.

Urbanek, R. E., C. K. Nielsen, T. S. Preuss, and G. A. Glowacki. 2012. Comparison of aerial surveys and pellet-based distance sampling methods for estimating deer density. Wildlife Society Bulletin 36:100–106.

U.S. Environmental Protection Agency. 1997. Level III ecoregions of the continental United States (revision of Omernik, 1987). Environmental Protection Agency—National Health and Environmental Effects Research Laboratory, Corvallis, Oregon, USA.

Vazquez, C., J. M. Rowcliffe, K. Spoelstra, and P. A. Jansen. 2019. Comparing diel activity patterns of wildlife across latitudes and seasons: time transformations using day length. Methods in Ecology and Evolution 10:2057–2066.

Wallace, B. P., A. D. DiMatteo, B. J. Hurley, E. M. Finkbeiner, A. B. Bolten, M. Y. Chaloupka, B. J. Hutchinson, F. A. Abreu-Grobois, D. Amorocho, K. A. Bjorndal, et al. 2010. Regional management units for marine turtles: a novel framework for prioritizing conservation and research across multiple scales. PLoS ONE 5(12):e15465.

Willi, M., R. T. Pitman, A. W. Cardoso, C. Locke, A. Swanson, A. Boyer, M. Veldthuis, and L. Fortson. 2019. Identifying animal species in camera trap images using deep learning and citizen science. Methods in Ecology and Evolution 10:80–91.

Williams, B. K., J. D. Nichols, and M. J. Conroy. 2002. Analysis and management of animal populations. Academic Press, San Diego, California, USA.

Winiarski, K. J., M. L. Burt, E. Rexstad, D. L. Miller, C. L. Trocki, P. W. Paton, and S. R. McWilliams. 2014. Integrating aerial and ship surveys of marine birds into a combined density surface model: a case study of wintering Common Loons. The Condor: Ornithological Applications 116:149–161.

Wood, D. H. 1988. Estimating rabbit density by counting dung pellets. Wildlife Research 15:665–671.

Zero, V. H., S. R. Sundaresan, T. G. O'Brien, and M. F. Kinnaird. 2013. Monitoring an endangered savannah ungulate, Grevy's zebra *Equus grevyi*: choosing a method for estimating population densities. Oryx 47:410–419.

Zipkin, E. F., E. R. Zylstra, A. D. Wright, S. P. Saunders, A. O. Finley, M. C. Dietze, M. S. Itter, and M. W. Tingley. 2021. Addressing data integration challenges to link ecological processes across scales. Frontiers in Ecology and the Environment 19:30–38.

Zuleger, A. M., R. Holland, and H. S. Kühl. 2022. Deriving observation distances for camera trap distance sampling. African Journal of Ecology 60:423–432.

Associate Editor: P. Schmidt.

SUPPORTING INFORMATION

Additional supporting material may be found in the online version of this article at the publisher's website.

How to cite this article: Delisle, Z. J., P. G. McGovern, B. G. Dillman, C. J. Reeling, J. N. Caudell, and R. K. Swihart. 2023. Using cost-effectiveness analysis to compare density-estimation methods for large-scale wildlife management. Wildlife Society Bulletin e1430. https://doi.org/10.1002/wsb.1430